A simple theoretical analysis of the burn-out times of an isothermal particle of coal char under air-firing, gasification and oxyfuel combustion in fluidised beds

Toyin Omojola*,&

Department of Engineering, Trumpington Street, University of Cambridge, Cambridge, CB2 1PZ, UK

& Current address: Department of Inorganic Chemistry, Fritz-Haber-Institut der Max-Planck-Gesellschaft. Berlin. D-14195. Germany.
* Corresponding author: toyin.omojola@bath.edu

Abstract

Coal combustion in air, gasification with carbon dioxide, and oxyfuel combustion in oxygen/carbon dioxide mixtures was studied at high process temperatures in a bubbling fluidised bed reactor where burning is controlled by external mass transfer conditions. Theoretical analysis of the burn-out times of an isothermal particle of coal char in air is provided for the case where a fraction of carbon monoxide is oxidized close to the char particle. Burn-out time equations are provided for the gasification of char in carbon dioxide. Both burn-out time equations are compared to analytical equations derived for the oxy-fuel combustion of char particles in oxygen/carbon dioxide mixtures. The results are particularly relevant for retrofitting existing bubbling fluidised bed reactors for clean energy generation to meet global warming targets.

1. Introduction

Increasing demand, security and sustainability are the global concerns for energy production in the 21st century. Currently, fossil fuels are still responsible for over 85% of energy demands [1]. Carbon dioxide, the product of coal combustion in coal fired powered stations, can be captured by various methods such as: post-combustion with a chemical wash, pre-combustion methods where gasification is combined with water gas shift reaction and oxy-fuel combustion where the fuel is burnt in oxygen/carbon dioxide mixtures in order to produce (after dehydration) a pure stream of carbon dioxide, which can be liquefied and made ready for transport and storage.

Of the energy technologies that could meet the target for on-purpose global warming reduction, carbon capture and storage could contribute significantly to purpose reduction of carbon dioxide produced from power plants. Once captured, carbon dioxide can be stored in deep saline aquifers. Deep saline aquifers have a larger storage capacity and can retain oxygen for a longer period of time. Carbon dioxide can also be used for enhanced oil recovery. Carbon dioxide storage is, however, beyond the scope of this research.

The higher concentrations of carbon dioxide and water during oxyfuel combustion leads to higher furnace gas emissivity and increase the radiative heat transfer in the furnace. Also, a higher density and specific heat capacity of carbon dioxide compared to nitrogen in air would require changes in the mass flow rates and velocities so as to attain similar adiabatic flame temperatures to the air firing situation [2-4]. The diffusivity of carbon dioxide in nitrogen is 0.8 times the diffusivity of oxygen in nitrogen and this property would affect mass and heat transfer characteristics subsequently affecting combustion rates, burnout time, particle temperatures and ignition temperatures [5].

With respect to oxygen diffusion into porous char particles and temperatures [6] defined three regimes of char combustion. At very higher temperatures in a bubbling fluidised bed reactor (zone III), maximum char combustion rate is attained and burning is controlled by the external diffusion of oxygen through the diffusion film surrounding the char particle. Char burning can be approximated as a shrinking particle model in a fluidised bed as the particle changes in size, but its apparent density stays constant. Mass transfer coefficients and subsequently Sherwood numbers can be obtained from this zone. For this burning regime, diffusion boundary layer models i.e. (single and double film) can be incorporated to account for the homogenous reactions occurring around the particle. The single film model suggested by Nusselt [7], allows for the oxidation of carbon to be controlled by a quiescent film around the carbon particle to produce carbon monoxide and carbon dioxide according to reactions I and II below. Arthur [8] after removing the masking effect of homogenous oxidation of carbon monoxide, observed carbon monoxide to be the primary product of char combustion above

1273 K. This work is confirmed by [9]. The double film model is activated at higher particle temperatures after which heat has been conducted and/or convected to the particle. Here, the burning rates are controlled by the carbon dioxide gasification of char. The activation of the double film burning mode could also depend on the reactivity of the char. The double film model was proposed by Burke and Schumann [10]. Carbon monoxide, primary product of char combustion reacts with oxygen in a thin flame front to produce carbon dioxide. Carbon dioxide further reacts with the carbon surface to produce carbon monoxide and simultaneously start the process over. Eventually, oxygen does not reach the surface of the carbon particle. Here, char burning rate depends on the gasification rate of carbon. Generally, a continuous model incorporating both single and double film models can be solved for different time frames of char combustion. This would involve solving partial differential equations with the transition from single film model to double film model at the temperature at which the gasification of char is activated on the particle surface [11]. Models can be made easier to solve if the double film model is ruled out subject to combustion rate exceeding the gasification rate in 100% carbon dioxide.

When char particles burn; the velocity, thermal and diffusion boundary layers are simultaneously developed and independent of each other. The thickness of these boundary layers change as combustion proceeds. Char particles burning in a fluidised bed are small enough such that laminar boundary layers are formed on combustion. Various models have been subjected into representing conditions in the region of phase boundaries between an immersed solid sphere and gas in a fluidised bed. These fall into three major categories: Whitman [12] suggested the steady state two film theory, where all resistance to mass transfer across a phase boundary can be regarded as lying in a thin film close to the interface. The transfer across this film can be regarded as a steady state process of molecular diffusion. Higbie [13] suggested the penetration theory such that the transfer process is largely attributable to fresh material being brought by eddies to the interface, where a process of unsteady state transfer took place for a fixed period at the freshly exposed surface. Danckwerts [14] modified the penetration theory to suggest the fresh material is kept at the surface for varying lengths of time and proposes a random age distribution of such elements for which the transfer is by an unsteady state process to the second phase. Finally, Toor and Marchello [15] have shown that all theories previously described are limiting cases of their own. Dennis et al. [16] have confirmed the suitability of film theory for characterizing mass transfer resistance. They further suggested the rejection of surface renewal models for char combustion in a fluidised bed.

All three factors (combustion, gasification, and carbon monoxide oxidation) are important in examining the influence of char conversion under oxyfuel conditions. Yet only, but a few studies have been carried out on oxyfuel combustion in fluidised beds. In this work,

we provide burn-out time equations for char burning under air firing, gasification and oxyfuel firing conditions.

2. Theory

2.1. Rates of oxyfuel combustion using the single film model

A model that accounts for the transport and reaction of oxygen on the char particle surface is modified, here for the added transport effect and reaction of carbon dioxide on the surface of the particle as experienced during oxyfuel combustion.

Four parallel processes are involved:

1. $r_1'(mol/s/particle) = \frac{2}{(1+\chi)}\pi d_p^2 K_{g,O2}\left(C_{p,O2} - C_{s,O2}\right)$ (2.1)
2. $r_2'(mol/s/particle) = \pi d_p^2 K_{g,CO2}\left(C_{p,CO2} - C_{s,CO2}\right)$ (2.2)
3. $r_3'(mol/s/particle) = \frac{\pi d_p^3}{6}\eta_{O2} K_{i,O2} C_{O2,s}$ (2.3)
4. $r_4'(mol/s/particle) = \frac{\pi d_p^3}{6}\eta_{CO2} K_{i,CO2} C_{CO2,s} = \frac{\pi d_p^3}{6} K_{v,CO2} C_{CO2,s}$ (2.4)

Also, the series production of carbon dioxide from combustion could have an additional influence on the surface gasification reactions, but for this model, this process is neglected.

For oxygen:

$$\frac{\pi d_p^3}{6}\eta_{O2} K_{i,O2} C_{O2,s} = \frac{2}{(1+\chi)}\pi d_p^2 K_{g,O2}\left(C_{p,O2} - C_{s,O2}\right)$$

$$C_{s,O2} = \frac{\left(\frac{2}{1+\chi}\right) K_{g,O2} C_{p,O2}}{\frac{d_p}{6}\eta_{O2} K_{i,o2} + \left(\frac{2}{1+\chi}\right) K_{g,O2}} \quad (2.5)$$

For carbon dioxide:

$$\frac{\pi d_p^3}{6} K_{v,CO2} C_{CO2,s} = \pi d_p^2 K_{g,CO2}\left(C_{p,CO2} - C_{s,CO2}\right)$$

$$C_{s,CO2} = \frac{K_{g,CO2} C_{p,CO2}}{\frac{d_p}{6} K_{v,CO2} + K_{g,CO2}} \quad (2.6)$$

Both surface reactions can be written:

$$r_5\ (mol/s/particle) = \frac{\pi d_p^3}{6}\left(K_{v,CO2} C_{CO2,s} + \eta_{O2} K_{i,O2} C_{O2,s}\right)$$

Further substituting the above equations into the surface reaction.

$$r_5 = \frac{\pi d_p^3}{6}\left(\frac{K_{v,CO2} K_{g,CO2} C_{p,CO2}}{\frac{d_p}{6} K_{v,CO2} + K_{g,CO2}} + \frac{\eta_{O2} K_{i,O2}\left(\frac{2}{1+\chi}\right) K_{g,O2} C_{p,O2}}{\frac{d_p}{6}\eta_{O2} K_{i,o2} + \left(\frac{2}{1+\chi}\right) K_{g,O2}}\right) \quad (2.7)$$

$$r_5'(mol/s/kg\ char) = \frac{1}{\rho_P}\frac{6}{d_p}\left(\frac{1}{\frac{1}{K_{g,CO2}}+\frac{6}{d_p}\frac{1}{K_{v,CO2}}}C_{p,CO2} + \frac{1}{\frac{(1+\chi)}{2K_{g,O2}}+\frac{6}{d_p}\frac{1}{K_{i,O2}\eta_{O2}}}C_{p,O2}\right) \quad (2.8)$$

Certain approximations can be made as lignite char is burned in the oxygen transfer controlled regime such that $C_{s,\,O2} \approx 0$ and $K_{i,O2} \gg K_{g,O2}$. The equation reduces to:

$$r_5' = \frac{1}{\rho_P}\frac{6}{d_p}\left(\frac{C_{p,CO2}}{\frac{1}{K_{g,CO2}}+\frac{6}{d_p}\frac{1}{K_{v,CO2}}} + \frac{2K_{g,O2}C_{p,O2}}{(1+\chi)}\right)$$

$$r_5' == \frac{1}{\rho_P}\frac{6}{d_p}\left(\frac{C_{p,CO2}}{\frac{d_p}{Sh_{CO2}D_{G,CO2}}+\frac{6}{d_p}\frac{1}{K_{v,CO2}}} + \frac{2Sh_{O2}D_{G,O2}C_{p,O2}}{d_p(1+\chi)}\right) \quad (2.9)$$

The final equation shows the contribution of the parallel char gasification reaction with carbon dioxide and combustion reaction with oxygen to char conversion. The model does not account for the series production of carbon dioxide and its consumption on the surface through gasification. The extent of external mass transfer of carbon dioxide and intraparticle mass transfer can be evaluated.

First, the effect of external mass transfer is calculated for the gasification of char in carbon dioxide. Sherwood number, $Sh_{CO2} \approx 1.66$ at 1000 °C for char particles of sizes (2.38 – 2.813 mm) using the following variables: $\varepsilon_{mf} = 0.44$, $U_{mf} = 0.0155$ m s^{-1}, $\nu = 1.18 \times 10^{-4}$ m^2 s^{-1}. $D_G = 1.87 \times 10^{-4}$ m^2 s^{-1}. The maximum rate of combustion is calculated as:

$$r_{max,CO2} = 2 \times 0.91 \times Sh \times D_{g,CO2} \times [CO_2]_{bulk} \times \frac{6}{\rho_e d_p^2} = 4.52\ mol\ s^{-1}\ kg_{char}^{-1}$$

This rate is much more than the observed rate of combustion in oxyfuel mixtures. At 800°C, $Sh_{CO2} \approx 1.84$ and $r_{max,CO2} = 2.44\ mol\ s^{-1}\ kg_{char}^{-1}$. For the maximum rates due to external transfer of oxygen through the film surrounding the particle, $Sh_{O2} \approx 1.60$

$$r_{max,O2} = 2 \times 0.91 \times Sh \times D_{g,O2} \times [O_2]_{bulk} \times \frac{6}{\rho_e d_p^2} = 1.15\ mol\ s^{-1}\ kg_{char}^{-1}.$$

At 800°C, $Sh_{O2} \approx 1.75$; $r_{max,O2} = 1.13\ mol\ s^{-1}\ kg_{char}^{-1}$

Air combustion rates are constant with temperature. The results show that external diffusion of carbon dioxide does not limit the conversion of char in the oxyfuel case.

The Laurendeau review [17] on various carbon dioxide gasification experiments reported activation energies of 230 to 280 kJ mol^{-1} for chars gasified between 875 – 1325 K in a fixed, fluidised bed or from thermogravimetric analysis and up to 370 kJ mol^{-1} for ultra-pure carbon. When char particles of size 2.38 – 2.813 mm are burned in air, activation energy of zero is obtained. However, when burned in oxyfuel mixtures, activation energies greater than 40 kJ mol^{-1} are obtained. Equation 2.7 is written to account for gasification and

combustion reactions on the surface of the char particle. It is evident that $\frac{d(\ln r_5')}{d(\frac{1}{T})}$ should predict activation energies. Differentiation of the logarithm of equation 2.9 vs 1/T will then provide an estimate of the effective activation energy, which can be compared with the experimentally observed value of 40 kJ mol^{-1}.

2.2. Boundary layer thickness

In the oxyfuel case, diffusivity is assumed to be equal to some mean value for $D_{O2,\,CO2}$ for 21% oxygen and 79 % carbon dioxide at 1000 °C. With d_p = 2.36 – 2.813 mm $D_{o2,Co2} = 1.87 \times 10^{-4}\ m^2 s^{-1}\ and\ D_{o2,N2} = 2.41 \times 10^{-4}\ m^2 s^{-1}$.

In order to obtain the mass transfer thickness, the Sherwood number is correlated from Hayhurst and Parmar [18] and correlated to the equations given by Paterson & Hayhurst [19]. Hayhurst's [20] correlation for d_p < 3mm, i.e. 2.36 – 2.813 mm:

$$Sh = \frac{K_g d_p}{D_g} = 2\varepsilon_{mf} + 0.61\left(\frac{U_p d_p}{\upsilon \varepsilon_{mf}}\right)^{0.48}\left(\frac{\nu}{D_g}\right)^{1/3} \qquad (2.10)$$

where D_g is the diffusivity of oxygen through carbon dioxide.

Particle velocity U_p is given as $U_{mf}\ (1-\varepsilon_b)\left\{1-\frac{\pi}{2}\ln\ (1-\frac{6\varepsilon_b}{\pi}\right\}$

where ε_b is the bubble voidage in the fluidised bed

$\varepsilon_b = \frac{U-U_{mf}}{U_B} = \frac{H-H_{mf}}{H}$

ν is the kinematic viscosity of the medium.

H and H_{MF} are the heights of the fluidised bed and the height at minimum fluidisation.

U is the superficial flow velocity and U_B represents the bubble rise velocity.

The bubble rise velocity, U_B, is given by:

$U_B = \left(U - U_{mf}\right) + 0.711(g d_b)^{0.5}$

where d_b is the mean bubble diameter.

The mean bubble diameter for a porous plate distributor and assuming that the mean size is 50% of the bubble size at height H above the bed is obtained from Darton et al. [21]:

$d_{b,m} = \frac{0.54(U-U_{mf})^{0.4}H^{0.8}}{2g^{0.2}}$

For oxyfuel mixtures (21% oxygen, 79% carbon dioxide), H_{mf} = 0.115 m and H ≈ 0.148 m, for a cold flowrate of Q = 20 L min^{-1}, U = 0.126 m s^{-1} at 1000°C. U_{mf} = 0.0155 m s^{-1} for inert sand particles of size, d_s = 0.215 mm and sand density = 2650 kg m^{-3}, $d_{b,m} = 0.0154\ m$, $U_B = 0.386\ m\ s^{-1}, \varepsilon_b \sim 0.33, U_p = 0.0264\ m\ s^{-1}$.

$For\ d_p = 0.0026\ m,\ \upsilon = 1.18 \times 10^{-4} m\ s^{-1}, D_e = 1.87 \times 10^{-4}\ m^2 s^{-1}.\ \varepsilon_{mf} = 0.44\ and\ Sh = 1.28.$

In both cases, the values of the film thickness can be obtained from $Sh = Sh_o\left(1+\frac{d_p}{2\delta}\right)$, where $Sh_o = 2\varepsilon_{mf}$ = 0.88. Accordingly, for char particles d_p = 2.38 – 2.813 mm, the film

thickness is $\delta_{air} = 2.82mm$ during oxyfuel combustion, and $\delta_{oxf} = 3.45mm$ during air combustion.

The boundary layer thickness is greater than the arithmetic mean of sand particles.

2.3. Char burn-out times under air firing

A full scale model that accounts for the chemistry of surface reactions, pore diffusion, film diffusion and the hydrodynamics of gas transfer between the bubble and the particulate phases is presented.

The following assumptions are made:

1. The two phase theory of fluidisation applies to the fluidised bed [22]. The bubble and particulate phases are considered.
2. The fluidised bed is isothermal during char combustion experiments.
3. Combustion of CO occurs in the bubble phase and in the freeboard [23]
4. The particulate phase approximates a well-mixed reactor.
5. The bubble phase moves in plug flow through the particulate phase.
6. The kinetics of reactions is modelled as first-order relations.
7. Gas passes through each bubble with volume; V has a volumetric flowrate, Q and has a rise velocity of U_b.
8. Interphase transport of gas is given by cross-flow factors, $X = QH/U_bV$.
9. Char is gasified to carbon monoxide in the particulate phase. A fraction of carbon monoxide is oxidised close to the char particle and the rest oxidised either in the bubble phase or in the freeboard.

The four reactions considered are:

$$C_{(s)} + ½O_{2\,(g)} \rightarrow CO_{\,(g)} \quad (2.3.1)$$

$$C_{(s)} + O_{2\,(g)} \rightarrow CO_{2\,(g)} \quad (2.3.2)$$

$$C_{(s)} + CO_{2\,(g)} \rightarrow 2CO_{\,(g)} \quad (2.3.3)$$

$$CO_{\,(g)} + ½\ O_{2\,(g)} \rightarrow CO_{2\,(g)} \quad (2.3.4)$$

Reaction step 2.3.3 is neglected for the determination of burnout times for char combustion under air-firing in fluidised beds. Determination of burnout times due to gasification of char is developed in section 2.4.

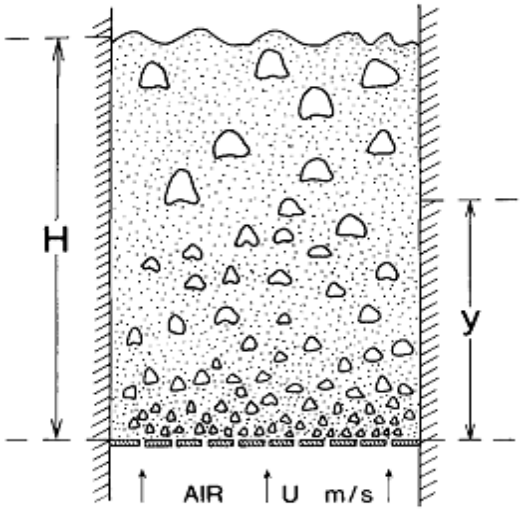

Figure 2.1: Schematic diagram of a bed of sand fluidised by air. Bubble size increases with height, y, up to the bed; in this model, this is ignored. Diagram obtained from Hayhurst [23].

Considering a single bubble of volume V_b in a bed; the bubble's rise velocity is:

$$U_b = \frac{dy}{dt} \; ; \frac{1}{dt} = \frac{U_b}{dy} \tag{2.11}$$

2.3.1. Mass balance on the bubbles

$$O_2: \quad \frac{dC_{bO2}}{dy} = \frac{Q}{U_b V_b}\left(C_{pO2} - C_{bO2} - \frac{C_{pCO}}{2}\right) \tag{2.12}$$

$$CO_2: \frac{dC_{bCO2}}{dy} = \frac{Q}{U_b V_b}\left(C_{pCO2} - C_{bCO2} + C_{PCO}\right) \tag{2.13}$$

The extra term in the expression for cross flow of oxygen (and carbon dioxide) arises by assuming carbon monoxide combusts instantaneously on entering bubble that carbon monoxide in $CO_{(g)} + ½\ O_{2\,(g)} \rightarrow CO_{2\,(g)}$.

Equation 2.12 can be integrated with initial condition $y = 0, C_{bo2} = C_{iO2}$ to obtain:

$$C_{b,O2} = C_{pO2} - \frac{C_{pCO}}{2} + \left[C_{i,O2} - C_{p,O2} + \frac{C_{pCO}}{2}\right] exp\left(\frac{-Qy}{U_b V_b}\right) \tag{2.14}$$

Equation 2.13 can also be integrated with initial condition at $y = 0, C_{bCO2} = 0$ to obtain:

$$C_{bCO2} = \left(C_{pCO2} + C_{pCO}\right)\left[1 - exp\left(\frac{-Qy}{U_b V_b}\right)\right] \tag{2.15}$$

2.3.2. Kinetics

Reaction 2.3.1 occurs in the particulate phase:

$$C_{(s)} + ½O_{2\,(g)} \rightarrow CO_{(g)} \qquad (2.3.1)$$

Char conversion in the particulate phase according to reaction 2.3.1 gives:

$$N_p r = N_b Q C_{pCO} \qquad (2.16)$$

where r is the rate of disappearance of carbon from one particle. N_p is the total number of char particles, N_b is the number of bubbles in the entire bed.

2.3.3. Evaluating rates

The rate of mass transfer of oxygen from the particulate phase to the external surface of the single spherical carbon particle is:

$$r_{O2} = \pi d_p^2 k_{g,O2}\left(C_{pO2} - C_{sO2}\right) \qquad (2.17)$$

However, the rate of oxidation of carbon is also affected by the ratio of the two possible products (carbon monoxide or carbon dioxide). If only carbon monoxide is formed at the carbon's surface and all carbon monoxide oxidation occurs far away from the particle either in the bulk of the bed or in the freeboard, the molar rate of oxygen consumption is given by:

$$r = 2r_{O2} = 2\pi d_p^2 k_{g,O2}\left(C_{pO2} - C_{sO2}\right) \qquad (2.18)$$

On the other hand, if only carbon dioxide is produced at the particle's surface, the rate of carbon oxidation is equal to the rate of oxygen consumption, such that

$$r = r_{O2} = \pi d_p^2 k_{g,O2}\left(C_{pO2} - C_{sO2}\right) \qquad (2.19)$$

Equations 2.18 and 2.19 represent the two extremes of the rate of carbon consumption. In this model, it is assumed that both carbon monoxide and carbon dioxide are formed close to the carbon particle and it is clear that the ratio of primary products carbon monoxide and carbon dioxide has a significant influence on the overall rate of combustion and needs to be known accurately [18]. The ratio of the primary products is known to depend on the temperature of the burning carbon particle, chemical reactivity of the resulting char and diameter of sand particles [24]. The overall rate of carbon oxidation is given in terms of χ, the proportion of carbon, which forms carbon dioxide at the particle surface. In this case, the reacting sphere produces (1 – χ)r mol/s of carbon monoxide and χr mol/s of carbon dioxide.

This requires: $(1-\chi)\,r/2 + \chi r = \frac{(1+\chi)r}{2} = \pi d_p^2 k_{g,O2}\left(C_{pO2} - C_{sO2}\right)$ and thus,

$$r = \frac{2}{(1+\chi)}\pi d_p^2 k_{g,O2}\left(C_{pO2} - C_{sO2}\right) \tag{2.20}$$

And also, with respect to oxidation on the surface of the carbon, assuming first-order reaction:

$$r = \pi d_p^2 k_{v,o2} C_{sO2} \tag{2.21}$$

Equations 2.20 and 2.21 can be combined to obtain

$$r = \pi d_p^2 C_{pO2}\left(\frac{1}{k_{v,O2}} + \frac{1+\chi}{2k_{g,O2}}\right)^{-1} = \pi d_p^2 K_{O2} C_{pO2} \tag{2.22}$$

$$\frac{1}{K_{O2}} = \frac{1}{k_{v,O2}} + \frac{1+\chi}{2k_{g,O2}} = \frac{1}{k_{v,O2}} + \frac{(1+\chi)d_p}{2Sh_{O2}D_{GO2}} \tag{2.23}$$

Also

$$r = -\frac{dm}{dt} = -\frac{\pi\rho_c d_p^2}{24}\frac{ddp}{dt} \tag{2.24}$$

Equation 2.22 and 2.24 can be combined to obtain

$$r = -\frac{dm}{dt} = -\frac{\pi\rho_c d_p^2}{24}\frac{dd_p}{dt} = \pi d_p^2 C_{pO2}\left(\frac{1}{k_{v,O2}} + \frac{1+\chi}{2k_{g,O2}}\right)^{-1} = \pi d_p^2 K_{O2} C_{pO2} \tag{2.25}$$

2.3.4. Mass Balance on the whole fluidised bed: oxygen

Assuming steady state in the fluidised bed, a mass balance for oxygen can be carried out on the fluidised bed:

$$N_p r = N_b Q C_{pCO}$$

$$r = -\frac{\pi\rho_c d_p^2}{24}\frac{dd_p}{dt}$$

$$\frac{N_p r}{2} = \frac{N_b Q C_{pCO}}{2} = -\frac{\pi\rho_c d_p^2}{48}\frac{dd_p}{dt}$$

$$AUC_{iO2} = A\left(U - U_{mf}\right)C_{bHO2} + AU_{mf}C_{PO2} + \frac{N_p r}{2} + \frac{N_b Q C_{pCO}}{2} - \frac{AU_{mf}C_{pCO}}{2} \tag{2.26}$$

The first term on the left represents the input into the system, the second and third terms on the right represent the output of the system and the last three terms represent consumption in the particulate, bubble phases and the freeboard. Equation 2.26 can be reduced to obtain:

$$UC_{iO2} = \left(U - U_{mf}\right)C_{bHO2} + U_{mf}C_{PO2} - \frac{N_p\pi\rho_c d_p^2}{24A}\frac{dd_p}{dt} - \frac{U_{mf}C_{pCO}}{2} \tag{2.27}$$

But from mass balance on the bubbles, equation 2.14 gives:

$$C_{b,O2} = C_{pO2} - \frac{C_{pCO}}{2} + \left[C_{i,O2} - C_{p,O2} + \frac{C_{pCO}}{2}\right] e^{\frac{-Qy}{U_b V_b}} \quad (2.14)$$

$At\ the\ bed\ surface;\ y = H;\ C_{b,O2} = C_{b,HO2}$

$$C_{b,HO2} = C_{i,O2} e^{-X} + \left(C_{pO2} - \frac{C_{pCO}}{2}\right)(1 - e^{-X}) \quad (2.28)$$

Inserting equation 2.28 into 2.27 gives:

$$C_{iO2} + \frac{C_{pCO}}{2} = C_{pO2} - \frac{N_p \pi \rho_c d_p^2}{24AY} \frac{dd_p}{dt} \quad (2.29)$$

$where\ Y = U - (U - U_{mf}) e^{-X}$

$$N_p r = N_b Q C_{pCO} = -\frac{N_P \pi \rho_c d_p^2}{24} \frac{dd_p}{dt};\ C_{pCO} = -\frac{N_P \pi \rho_c d_p^2}{24 N_b Q} \frac{dd_p}{dt};\ \frac{C_{pCO}}{2} = -\frac{N_P \pi \rho_c d_p^2}{48 N_b Q} \frac{dd_p}{dt}$$

From equation 2.25:

$$r = -\frac{dm}{dt} = -\frac{\pi \rho_c d_p^2}{24} \frac{dd_p}{dt} = \pi d_p^2 C_{pO2} \left(\frac{1}{k_{v,O2}} + \frac{1+\chi}{2k_{g,O2}}\right)^{-1} = \pi d_p^2 K_{O2} C_{pO2} \quad (2.25)$$

$$C_{pO2} = -\frac{\rho_c}{24 K_{O2}} \frac{ddp}{dt} = -\frac{\rho_c}{24} \left\{\frac{1}{k_{v,O2}} + \frac{1+\chi}{2k_{g,O2}}\right\} \frac{ddp}{dt} \quad (2.30)$$

Substituting $\frac{C_{pCO}}{2}$ and C_{pO2} gives:

$$C_{iO2} = -\frac{\rho_c}{24} \left[\frac{1}{k_{v,O2}} + \frac{(1+\chi) d_p}{2Sh_{O2} D_{G,O2}} + \frac{N_p \pi d_p^2}{AY} (1 - \alpha)\right] \frac{ddp}{dt}\ \alpha = \frac{AY}{2N_b Q} \quad (2.31)$$

Equation 2.31 gives the rate of change of particle diameter with time. This equation can be integrated with initial conditions at t = 0, $d_p = d_o$, and assuming that k does not vary with time to obtain:

$$\frac{24 C_{iO2} t}{\rho_c} = \frac{d_o}{k_{v,O2}} + \frac{(1+\chi) d_o^2}{4Sh_{O2} D_{G,O2}} + \frac{N_p \pi d_o^3}{3AY} (1 - \alpha) - \frac{d_p}{k_{v,O2}} - \frac{(1+\chi) d_p^2}{2Sh_{O2} D_{G,O2}} - \frac{N_p \pi d_p^3}{3AY} (1 - \alpha) \quad (2.32)$$

The burnout time of char particle, $t_{b,O2}$, is evaluated at $d_p = 0$ such that:

$$\frac{24 C_{iO2} t_{b,O2}}{\rho_c} = \frac{d_o}{k_{v,O2}} + \frac{(1+\chi) d_o^2}{4Sh_{O2} D_{G,O2}} + \frac{N_p \pi d_o^3}{3AY} (1 - \alpha)$$

$$t_{b,O2} = \frac{\rho_c d_o}{24 C_{iO2} k_{v,O2}} + \frac{(1+\chi) d_o^2 \rho_c}{96 Sh_{O2} D_{G,O2} C_{iO2}} + \frac{N_p \pi d_o^3 \rho_c (1 - \alpha)}{72 AY C_{iO2}} \quad (2.33)$$

Also, the mass of a batch of char particles, m_a

$$m_a = \frac{N_p \pi d_o^3 \rho_c}{6 w_c};\ m_a w_c = \frac{N_p \pi d_o^3 \rho_c}{6}$$

Therefore:

$$t_{b,O2} = \frac{\rho_c d_o}{24 k_{v,O2} C_{iO2}} + \frac{(1+\chi) d_o^2 \rho_c}{96 Sh_{O2} D_{G,O2} C_{iO2}} + \frac{m_a w_c (1-\alpha)}{12 A Y C_{iO2}} \quad (2.34)$$

Equation 2.34 differs from the correlation for burnout time derived by Hayhurst [23] as this accounts for χ, the fraction of carbon monoxide that oxidises to carbon dioxide at the particle surface.

2.4. Burn-out time during char gasification

Here, just one reaction is considered:

$C_{(s)} + CO_{2\,(g)} \rightarrow 2CO_{(g)}$ (2.3.3)

This reaction is assumed to occur in the particulate phase as the char particles are resident there to produce bubbles of carbon monoxide which rise through the bed and exit through the flue gas. No reaction occurs in the bubble phase.

2.4.1. Mass balance on the bubbles: carbon monoxide and carbon dioxide

Carbon monoxide	Carbon dioxide
$\frac{dC_{bCO}}{dy} = \frac{Q}{U_b V_b}(C_{pCO} - C_{bCO})$	$\frac{dC_{bCO2}}{dy} = \frac{Q}{U_b V_b}(C_{pCO2} - C_{bCO2})$
$C_{bCO} e^{\frac{Qy}{U_b V_b}} = C_{pCO} e^{\frac{Qy}{U_b V_b}} + M$	$C_{bCO2} e^{\frac{Qy}{U_b V_b}} = C_{pCO2} e^{\frac{Qy}{U_b V_b}} + N$
$At\ y = 0; C_{bCO} = 0\ ; M = -C_{pCO}$	$At\ y = 0; C_{bCO2} = C_{iCO2}\ ; N = C_{iCO2} - C_{pCO2}$
$C_{bCO} e^{\frac{Qy}{U_b V_b}} = C_{pCO} e^{\frac{Qy}{U_b V_b}} - C_{pCO}$	$C_{bCO2} e^{\frac{Qy}{U_b V_b}} = C_{pCO2} e^{\frac{Qy}{U_b V_b}} + C_{iCO2} - C_{pCO2}$
$C_{bCO} = C_{pCO} - C_{pCO} e^{-\frac{Qy}{U_b V_b}}$ (2.35)	$C_{bCO2} = C_{pCO2} + [C_{iCO2} - C_{pCO2}] e^{-\frac{Qy}{U_b V_b}}$ (2.36)

$At\ the\ bed\ surface; y = H;\ C_{bCO} = C_{bHCO}\ \&\ C_{bCO2} = C_{bHCO2}\ ; crossflow\ factor, X = \frac{QH}{U_b V_b}$

$C_{bHCO} = C_{pCO} - C_{pCO} e^{-X}$ (2.37)	$C_{bHCO2} = C_{pCO2} + [C_{iCO2} - C_{pCO2}] e^{-X}$ (2.38)

Table 2.1: Mass balance carbon monoxide and carbon dioxide in the bubble phase

2.4.2. Kinetics of char gasification with carbon dioxide

The rate of mass transfer of carbon dioxide to the surface of the char particle is given by:

$$r = r_{CO2} = \pi d_p^2 k_{g,CO2}\left(C_{pCO2} - C_{sCO2}\right) \tag{2.39}$$

Also, assuming first order kinetics, the rate of char gasification is given by:

$$r = \pi d_p^2 k_{v,Co2} C_{sCO2} \tag{2.40}$$

Combining equations 2.39 and 2.40:

$$C_{PCO2} = \frac{r}{\pi d_p^2}\left(\frac{1}{k_{v,CO2}} + \frac{1}{k_{g,CO2}}\right) = \frac{r}{\pi d_p^2}\left(\frac{1}{k_{v,CO2}} + \frac{d_p}{Sh_{CO2} D_{G,CO2}}\right)$$

$$r = \pi d_p^2 C_{pCO2}\left(\frac{1}{k_{v,CO2}} + \frac{d_p}{Sh_{CO2} D_{G,CO2}}\right)^{-1} = \pi d_p^2 K_{CO2} C_{pCO2} \tag{2.41}$$

$$\frac{1}{K_{CO2}} = \frac{1}{k_{v,CO2}} + \frac{d_p}{Sh_{CO2} D_{G,CO2}}$$

Assuming that the char particle shrinks at constant density,

$$r = -\frac{dm}{dt} = -\frac{\pi \rho_c d_p^2}{24}\frac{ddp}{dt} = \pi d_p^2 C_{pCO2}\left(\frac{1}{k_{v,CO2}} + \frac{d_p}{Sh_{CO2} D_{G,CO2}}\right)^{-1} = \pi d_p^2 K_{CO2} C_{pCO2}$$

$$C_{pCO2} = -\frac{\rho_c}{24}\left(\frac{1}{k_{v,CO2}} + \frac{d_p}{Sh_{CO2} D_{G,CO2}}\right)\frac{ddp}{dt} \tag{2.42}$$

Also

$$N_p r = 2 N_b Q C_{pCO}$$

For every mole of carbon consumed, two moles of carbon monoxide are produced according to reaction step 2.3.3.

2.4.3. Mass Balance on the whole fluidised bed: carbon dioxide

Assuming steady state in the fluidised bed and negligible gasification in the freeboard: One obtains:

$$AUC_{iCO2} = A\left(U - U_{mf}\right)C_{bHCO2} + AU_{mf} C_{PCO2} + N_p r \tag{2.43}$$

The first term on the left represents the input into the system, while the first two terms on the right gives the output of the bed at y = H. The last term on the right gives the consumption in the particulate phase, equation 2.42 can be reduced to obtain:

$$N_p r = -\frac{N_p \pi \rho_c d_p^2}{24}\frac{ddp}{dt}$$

$$C_{iCO2} = C_{pCO2} - \frac{N_p \pi \rho_c d_p^2}{24AY}\frac{ddp}{dt}, \qquad Y = U - \left(U - U_{mf}\right)e^{-X} \tag{2.45}$$

$$C_{pCO2} = -\frac{\rho_c}{24}\left(\frac{1}{k_{v,CO2}} + \frac{d_p}{Sh_{CO2}D_{G,CO2}}\right)\frac{ddp}{dt} \tag{2.46}$$

Consequently,

$$C_{iCO2} = -\frac{\rho_c}{24}\left\{\frac{1}{k_{v,CO2}} + \frac{d_p}{Sh_{CO2}D_{G,CO2}} + \frac{N_p \pi d_p^2}{AY}\right\}\frac{ddp}{dt} \tag{2.47}$$

Integrating the equation above with initial condition, $At\ t = 0, d_p = d_o$

$$\frac{24C_{iCO2}t}{\rho_c} = \left\{\frac{d_o - d_p}{k_{v,CO2}} + \frac{d_o^2 - d_p^2}{2Sh_{CO2}D_{G,CO2}} + \frac{N_p\pi\left(d_o^3 - d_p^3\right)}{3AY}\right\} \tag{2.48}$$

The burnout of a char particle under gasification conditions is obtained at $t = t_{b,CO2}, d_p = 0$

$$\frac{24C_{iCO2}t_{b,CO2}}{\rho_c} = \frac{d_o}{k_{v,CO2}} + \frac{d_o^2}{2Sh_{CO2}D_{G,CO2}} + \frac{N_p\pi d_o^3}{3AY}$$

$$t_{b,CO2} = \frac{\rho_c d_o}{24C_{iCO2}k_{v,CO2}} + \frac{\rho_c d_o^2}{48C_{iCO2}Sh_{CO2}D_{G,CO2}} + \frac{N_p\rho_c\pi d_o^3}{72C_{iCO2}AY} \tag{2.49}$$

$$m_a = \frac{N_p\pi d_o^3\rho_c}{6w_c}$$

$$m_a w_c = \frac{N_p\pi d_o^3\rho_c}{6}$$

$$t_{b,CO2} = \frac{\rho_c d_o^2}{48C_{iCO2}Sh_{CO2}D_{G,CO2}} + \frac{\rho_c d_o}{24C_{iCO2}k_{v,CO2}} + \frac{m_a w_c}{12AYC_{iCO2}} \tag{2.50}$$

But

$$t_{b,O2} = \frac{\rho_c d_o}{24k_{v,O2}C_{iO2}} + \frac{(1+\chi)d_o^2\rho_c}{96Sh_{O2}D_{G,O2}C_{iO2}} + \frac{mw_c(1-\alpha)}{12AYC_{iO2}} \tag{2.34}$$

2.5. Burn-out times with oxy-fuel mixtures

Here, four reactions are considered simultaneously. In the particulate phase: gasification to carbon monoxide occurs through:

$C_{(s)} + ½O_{2\,(g)} \rightarrow CO_{\,(g)}$ (2.4.1)

$C_{(s)} + CO_{2\,(g)} \rightarrow 2CO_{\,(g)}$ (2.4.2)

A fraction of carbon monoxide ,χ, oxidises close to the char particle in the particulate phase giving

$C_{(s)} + O_{2\,(g)} \rightarrow CO_{2\,(g)}$ (2.4.3)

While a fraction, $1 - \chi$, oxidises through equation 2.4.4 in the bubble phase and freeboard of the fluidised bed:

$CO_{\,(g)} + ½\ O_{2\,(g)} \rightarrow CO_{2\,(g)}$ (2.4.4)

We present here burn-out time equations for direct high-temperature oxyfuel combustion of char in a fluidised bed.

2.5.1. Kinetics

The kinetics of oxy-fuel combustion is given by equations 2.4.1 to 2.4.3. Rates of consumption of char is given as:

$$R_c = r_1 + r_2 + r_3 \tag{3.51}$$

If we assume direct char combustion to carbon dioxide under oxyfuel conditions, equation 2.51 becomes:

$$R_c = r_2 + r_3 \tag{2.52}$$

With two active species (oxygen, carbon dioxide) attacking the char particle, the rate of mass transfer to the surface of the char particle is given as:

$$r_{CO2} = \pi d_p^2 k_{g,CO2}\left(C_{pCO2} - C_{sCO2}\right)$$

$$r_{O2} = \pi d_p^2 k_{g,O2}\left(C_{pO2} - C_{sO2}\right)$$

If the rate of transfer of the two species equals the rate of char combustion, then:

$$\pi d_p^2\left[k_{g,O2}\left(C_{pO2} - C_{sO2}\right) + k_{g,CO2}\left(C_{pCO2} - C_{sCO2}\right)\right] = \pi d_p^2\left(k_{v,O2}C_{s,O2} + K_{v,CO2}C_{s,CO2}\right)$$

$$C_{s,CO2} = \frac{k_{g,O2}C_{pO2} + k_{g,CO2}C_{pCO2} - C_{s,O2}\left(k_{g,O2} + k_{v,O2}\right)}{k_{g,CO2} + k_{v,CO2}}$$

$$R_c = \pi d_p^2\left(k_{v,O2}C_{s,o2} + k_{v,CO2}\left(\frac{k_{g,O2}C_{pO2} + k_{g,CO2}C_{pCO2} - C_{s,O2}\left(k_{g,O2} + k_{v,O2}\right)}{k_{g,CO2} + k_{v,CO2}}\right)\right)$$

If we further assume that the combustion reaction (with oxygen) is quite fast at high temperatures such that: $C_{s,O2} \sim 0$ and $k_{v,CO2} \gg k_{g,CO2} \gg k_{g,O2}$ we obtain:

$$R_c = \pi d_p^2\left(k_{g,O2}C_{pO2} + k_{g,CO2}C_{pCO2}\right) \tag{2.53}$$

At high temperatures, the char particle shrinks at constant density according to:

$$r = -\frac{dm}{dt} = -\frac{\pi\rho_c d_p^2}{24}\frac{ddp}{dt} = \pi d_p^2\left(k_{g,O2}C_{pO2} + k_{g,CO2}C_{pCO2}\right)$$

$$C_{p,CO2} = -\left[\frac{\rho_c}{24k_{g,CO2}}\frac{d\left(d_p\right)}{dt} + \frac{k_{g,O2}}{k_{g,CO2}}\right] \sim -\frac{\rho_c}{24k_{g,CO2}}\frac{d\left(d_p\right)}{dt} \tag{2.54}$$

At high temperature, we have reaction steps 2.4.2 and 2.4.3 occurring, but only 2.4.2. is limiting and as such, similar conditions may occur as when the mass balance applies only to char gasification described in section 2.4:

$$C_{iCO2} = C_{pCO2} - \frac{N_p \pi \rho_c d_p^2}{24AY}\frac{ddp}{dt}, \qquad Y = U - \left(U - U_{mf}\right)e^{-X} \tag{2.45}$$

$$C_{iCO2} - \frac{\rho_c}{24}\left[\frac{1}{k_{g,CO2}} + \frac{N_p \pi d_p^2}{AY}\right]\frac{d\left(d_p\right)}{dt} \tag{2.55}$$

Integrating equation 2.55 with initial condition, $At\ t = 0, d_p = d_o$

$$\frac{24C_{iCO2}t}{\rho_c} = \left\{\frac{d_o - d_p}{k_{g,CO2}} + \frac{N_p \pi\left(d_o^3 - d_p^3\right)}{3AY}\right\} \tag{2.56}$$

The burnout of a char particle under oxyfuel conditions is obtained at $t = t_{b,O2/CO2}, d_p = 0$

$$\frac{24C_{iCO2}t_{b,O2/CO2}}{\rho_c} = \frac{d_o}{k_{g,CO2}} + \frac{N_p \pi d_o^3}{3AY}$$

$$t_{b,O2/CO2} = \frac{\rho_c d_o}{24C_{iCO2}k_{g,CO2}} + \frac{N_p \rho_c \pi d_o^3}{72C_{iCO2}AY} \tag{2.57}$$

$$m_a = \frac{N_p \pi d_o^3 \rho_c}{6w_c}$$

$$m_a w_c = \frac{N_p \pi d_o^3 \rho_c}{6}$$

The burn-out time for oxy-fuel combustion of char at high temperatures is:

$$t_{b,O2/CO2} = \frac{\rho_c d_o}{24C_{iCO2}k_{g,CO2}} + \frac{m_a w_c}{12AYC_{iCO2}} \tag{2.58}$$

We note that:

$$t_{b,O2} = \frac{\rho_c d_o}{24k_{v,O2}C_{iO2}} + \frac{(1+\chi)d_o^2 \rho_c}{96Sh_{O2}D_{G,O2}C_{iO2}} + \frac{mw_c(1-\alpha)}{12AYC_{iO2}} \tag{2.34}$$

$$t_{b,CO2} = \frac{\rho_c d_o^2}{48C_{iCO2}Sh_{CO2}D_{G,CO2}} + \frac{\rho_c d_o}{24C_{iCO2}k_{v,CO2}} + \frac{m_a w_c}{12AYC_{iCO2}} \tag{2.50}$$

For the first time, we present the analytical equations representing char burning under air (equation 2.34), gasification conditions (equation 2.50) and under oxyfuel conditions (equation 2.58) at high temperatures.

3. Conclusions

Theoretical equations for the burn-out times of char under air firing, oxyfuel firing, and under gasification conditions are considered in bubbling fluidised bed reactors at high process temperatures.

4. Acknowledgements

Toyin Omojola would like to thank Dr. Stuart Scott and Professor Nick Collings from the Department of Engineering at the University of Cambridge. Financial support from the Cambridge Commonwealth Trust (10140618) is also acknowledged.

5. References

1. Rathnam, R.K., et al. Fuel Processing Technology. 2009. **90**(6). 797-802.
2. Wall, T.F. Proceedings of the Combustion Institute. 2007. **31**(1). 31-47.
3. Buhre, B.J.P., et al. Progress in Energy and Combustion Science. 2005. **31**(4). 283-307.
4. Tan, Y., et al. Fuel. 2006. **85**(4). 507-512.
5. Oka, S.N., *Fundamental Processes during Fluidized Bed Combustion*, in *Fluidized Bed Combustion*, E.J. Anthony, Editor. 2004.
6. Walker, J., et al., in *Advances in Catalysis*, D.D. Eley, P. Selwood, and P.B. Weisz, Editors. 1959.
7. Nusselt, W. Verein Deutscher Ingenier. 1924. **68**. 124.
8. Arthur, J.R. Trans. Faraday Soc. . 1951. **47**(164).
9. Basu, P., et al., *Combustion of single coal particles in fluidized beds*, in *Fluidized Combustion*. 1975, The Institute of Fuel: London, United Kingdom.
10. Burke, S., et al. Proc. 3rd Int. Conf. Bituminous Coal. 1931. **2**. 485.
11. Kulasekaran, S., et al. Fuel. 1998. **77**(14). 1549-1560.
12. Whitman, W. Chem. and Met. Eng. . 1923. **29.** . 147.
13. Higbie, R. Trans. Am. Inst. Chem. Eng. . 1935. **31**. 365.
14. Danckwerts, P.V. Ind. Eng. Chem. . 1951. **43**. 1460.
15. Toor, H., et al. AIChE Journal. 1958. **4**. 97.
16. Dennis, J.S., et al. Combustion and Flame. 2006. **147**(3). 185-194.
17. Laurendeau, N.M. Prog. Energy Combustion Science. 1978. **4**. 221-270.
18. Hayhurst, A.N., et al. Combustion and Flame. 2002. **130**. 361-375.
19. Paterson, W.R., et al. Chemical Engineering Science. 2000. **55**. 1925-1927.
20. Hayhurst, A.N. Combustion and Flame. 2000. **121**. 679-688.
21. Darton, R.C., et al. Trans Inst Chem Eng. 1977. **55**(4). 274-280.
22. Davidson, J.F., et al. 1971((AUGUST, 1971)).
23. Hayhurst, A.N. Combustion and Flame. 1991. **85**. 155-168.
24. Hayhurst, A.N., et al. Chemical Engineering Science. 1998. **53**(3). 427-438.